Chemosphere 341 (2023) 140047

Contents lists available at ScienceDirect

Chemosphere

journal homepage: www.elsevier.com/locate/chemosphere

Sustainable reuse of toxic spent granular activated carbon by heterogeneous fenton reaction intensified by temperature changes

Andrés Sánchez-Yepes [a], Aurora Santos [a], Juana M. Rosas [b], José Rodríguez-Mirasol [b], Tomás Cordero [b], David Lorenzo [a,*]

[a] Chemical Engineering and Materials Department, Complutense University of Madrid, Spain
[b] Universidad de Málaga, Andalucia Tech., Departamento de Ingeniería Química, Campus de Teatinos S/n, 29010, Málaga, Spain

HIGHLIGHTS

- Iron and 124-TCB adsorption on GAC decrease the unproductive H_2O_2 consumption.
- The higher the iron adsorbed, the higher the oxidant.
- The higher the iron adsorbed, the higher adsorption capacity recovery.
- A positive effect of temperature on GAC regeneration is found up to 60 °C.
- GAC surface stable during the regeneration cycles with negligible iron leaching.

GRAPHICAL ABSTRACT

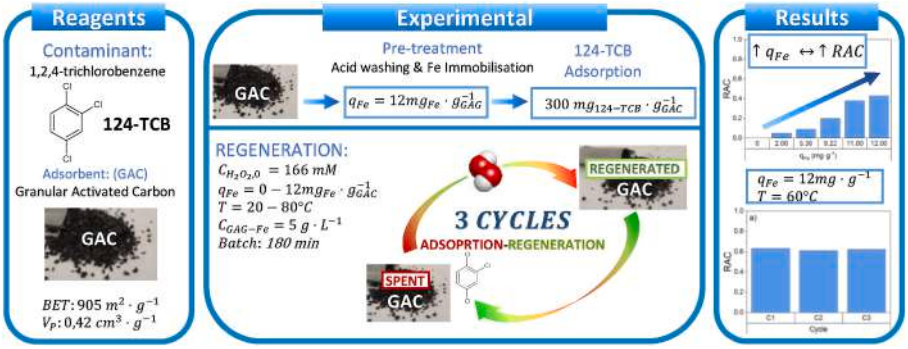

ARTICLE INFO

Handling Editor: Jun Huang

Keywords:
Heterogeneous fenton
Adsorption
Regeneration
Activated carbon
Chlorinated organic compounds

ABSTRACT

A common strategy for removing highly toxic organic compounds, such as chlorinated organic compounds, is their adsorption on granular activated carbon. Spent granular activated carbon results in a toxic residue to manage; therefore, the regeneration and reuse of granular activated carbon on the site would be advisable. This work studies the regeneration of a granular activated carbon saturated in 1,2,4-trichlorobenzene, chosen as the model chlorinated organic compounds, by heterogeneous Fenton, where iron was previously immobilised on the granular activated carbon surface. This methodology avoids the addition of iron to the aqueous phase at concentrations above the allowable limits and the need for acidification. Three successive cycles of adsorption-regeneration were carried out batchwise (5 $g_{GAC} \cdot L^{-1}$) with a granular activated carbon saturated with 300 $mg_{124\text{-}TCB} \cdot g_{GAC}^{-1}$. The recovery of the adsorption capacity after regeneration was studied with H_2O_2 (166 mM, 1.5 the stoichiometric dosage), at different concentrations adsorbed with iron adsorbed concentrations (0–12 $mg_{Fe} \cdot g_{GAC}^{-1}$) and temperatures (20–80 °C). Stable recovery of the adsorption capacity values of 65% were obtained at 180 min with 12 $mg_{Fe} \cdot g_{GAC}^{-1}$ and 60 °C. The porosity and surface chemistry of the adsorbent remained very similar after different adsorption-regeneration cycles without iron leaching into the aqueous phase. The oxidant consumption was close to the stoichiometric value for the mineralization of 1, 2, 4 – trichlorobenzene, with a low unproductive consumption of H_2O_2 with granular activated carbon. In addition, no aromatic or chlorinated by-

* Corresponding author.
E-mail address: dlorenzo@quim.ucm.es (D. Lorenzo).

https://doi.org/10.1016/j.chemosphere.2023.140047
Received 23 March 2023; Received in revised form 20 July 2023; Accepted 31 August 2023
Available online 1 September 2023

products were detected in the aqueous solution obtained in the regeneration process. The negligible toxicity of the aqueous phase with the Microtox bioassay confirmed the absence of toxic oxidation by-products.

1. Introduction

The presence of persistent organic pollutants (POPs), particularly chlorinated organic compounds (COCs), in wastewater, surface waters, and groundwater is a significant environmental problem to solve (Rodan et al., 1999; Klecka et al., 2000; Gramatica et al., 2002; Gramatica and Papa, 2007; Lougheed, 2007). Adsorption on granular activated carbon (GAC) is a common treatment to remove these compounds from the aqueous phase (Weber and Vanvliet, 1981; Alben et al., 1983; Marsh and Rodríguez-Reinoso, 2006a, 2006b; Zhang et al., 2021). The main drawback of POPs adsorption on GAC is that large amounts of contaminated carbon are generated. Spent GAC has often been regenerated by off-site thermal treatments at 800–1000 °C (San Miguel et al., 2002; Salvador et al., 2015; Baghirzade et al., 2021), with remarkable costs and losses of GAC mass. Furthermore, if the POPs adsorbed on the spent GAC are COCs (Urano et al., 1991; Bembnowska et al., 2003; Sanchez-Yepes et al., 2022), the GAC requires particular management.

Recently, advanced oxidation processes (AOP) have been studied to regenerate spent GAC, removing the pollutant adsorbed on the carbon surface (Huling et al., 2000, 2005, 2011; Toledo et al., 2003; Horng and Tseng, 2008; Huling and Hwang, 2010; Anfruns et al., 2013; Li et al., 2013; Cabrera-Codony et al., 2015; Plakas and Karabelas, 2016; Chen et al., 2017; Jatta et al., 2019; Peng et al., 2019; Cai et al., 2020; Crincoli et al., 2020; Ma et al., 2020; Santos et al., 2020; Xiao et al., 2020; Sanchez-Yepes et al., 2022). Persulfate (PS) (Huling et al., 2011; Jatta et al., 2019; Peng et al., 2019; Xiao et al., 2020; Sanchez-Yepes et al., 2022) or hydrogen peroxide (Huling et al., 2000, 2005; Toledo et al., 2003; Horng and Tseng, 2008; Huling and Hwang, 2010; Anfruns et al., 2013; Li et al., 2013; Cabrera-Codony et al., 2015; Plakas and Karabelas, 2016; Chen et al., 2017; Cai et al., 2020; Crincoli et al., 2020; Ma et al., 2020; Santos et al., 2020) have been used as oxidants.

GAC regeneration has also been studied using hydrogen peroxide catalysed by iron cation (Fenton reagent) to produce hydroxyl radicals OH· (Huling et al., 2000, 2005; Toledo et al., 2003; Horng and Tseng, 2008; Huling and Hwang, 2010; Anfruns et al., 2013; Li et al., 2013; Cabrera-Codony et al., 2015; Plakas and Karabelas, 2016; Chen et al., 2017; Cai et al., 2020; Crincoli et al., 2020; Ma et al., 2020; Santos et al., 2020).·Hydrogen peroxide and iron can be added simultaneously in the aqueous solution (Toledo et al., 2003; Huling et al., 2005; Horng and Tseng, 2008; Anfruns et al., 2013; Li et al., 2013; Chen et al., 2017; Cai et al., 2020; Crincoli et al., 2020; Ma et al., 2020; Santos et al., 2020), or iron can be previously adsorbed on the GAC (Huling et al., 2000; Huling and Hwang, 2010; Cabrera-Codony et al., 2015; Plakas and Karabelas, 2016).

Fenton Reagent (aqueous solution containing Fe cation and H_2O_2) has been used to regenerate spent GAC (Huling et al., 2000, 2005; Toledo et al., 2003; Horng and Tseng, 2008; Huling and Hwang, 2010; Anfruns et al., 2013; Li et al., 2013; Cabrera-Codony et al., 2015; Plakas and Karabelas, 2016; Chen et al., 2017; Cai et al., 2020; Crincoli et al., 2020; Ma et al., 2020; Santos et al., 2020) with adsorbed toluene (Ma et al., 2020), methyl *tert*-butyl ether (Huling et al., 2005), limonene (Anfruns et al., 2013), methylene blue (Santos et al., 2020), dyeing wastewater (Chen et al., 2017), etc. A representative work is that of Ma et al. (2020) regenerating a spent activated carbon (AC) with adsorbed toluene (512.25 $mg_{tol}\cdot g_{AC}^{-1}$) using a toluene/oxidant/Fe molar ratio of 1/20/1. A recovery of adsorption capacity between 85.6 and 84.9% was obtained after 6 cycles of adsorption-regeneration (regeneration time of each cycle of 3 h). Chen et al. (2017) treated a spent AC for tertiary treatment of dyeing wastewater (240 mg g^{-1}) with a molar ratio oxidant/Fe of 20/1. They achieved less than 50% of the recovery of the adsorption capacity after 7 regeneration cycles. The main drawback is that the use of Fenton reagent required acidic pH and a relatively high ratio of Fe to peroxide (Fe: H_2O_2 about 1:20), resulting in an iron concentration in the aqueous phase over the allowed discharged values.

The immobilisation of iron on the GAC surface has been proposed to avoid the presence of iron in the aqueous phase and the acidification of the reaction media (Huling et al., 2000; Huling and Hwang, 2010; Cabrera-Codony et al., 2015; Plakas and Karabelas, 2016). Huling et al. (2000) treated a spent GAC saturated in 2-chlorophenol (2-CP) (119 $mg_{2\text{-}CP}\cdot g_{GAC}^{-1}$), using GAC with adsorbed iron (9.8 $mg_{Fe}\cdot g_{GAC}^{-1}$) and an aqueous solution of H_2O_2 (2.1 M) at pH 4.6 and molar ratio pollutant: oxidant: Fe of 1:64:0.2. A recovery of the GAC adsorption capacity of 76% was obtained after three successive cycles of 24 h (Huling et al., 2000). Huling and Hwang (2010) also treated a spent AC with methyl *tert*-butyl ether (MTBE) (60 $mg_{MTBE}\cdot g_{GAC}^{-1}$) using adsorbed iron on GAC (8.75 $mg_{Fe}\cdot g_{GAC}^{-1}$) and an aqueous solution of H_2O_2 (0.49 mM). Recovery of adsorption capacity up to 70% was obtained at 24 h, using a pollutant: oxidant: Fe molar ratio of 1:17:0.2 (pH was kept between 2 and 4). Cabrera-Codony et al. (2015) studied the regeneration of a spent GAC with adsorbed octamethylcyclotetrasiloxane (1732 $mg_{OMCTX}\cdot g_{GAC}^{-1}$) using adsorbed iron (11.5 $mg_{Fe}\cdot g_{GAC}^{-1}$) and an aqueous solution of H_2O_2 (29 mM) for 24 h (without pH control). A decrease in adsorption capacity from 92.1% to 46.3% was reported after three cycles of adsorption-regeneration, using a molar ratio pollutant:oxidant:Fe of 1:20:0.04,. This decrease was associated with the loss of adsorbed iron in successive cycles. Plakas and Karabelas (2016) studied the regeneration of a spent AC saturated in diclofenac (DCF) (203 $mg_{DFC}\cdot g_{GAC}^{-1}$) using iron adsorbed on GAC (40.7 $mg_{Fe}\cdot g_{GAC}^{-1}$) as the catalyst and an aqueous solution of H_2O_2 3.5 mM as the oxidant, at neutral pH. A recovery of the adsorption capacity was obtained at 24 h of oxidation treatment (only one cycle was studied), using a pollutant: oxidant molar ratio: Fe of 1:73:1. These works have only studied the regeneration process at room temperature, and the effect of temperature on the process was not considered. Moreover, the oxidant consumption, changes in the physicochemical carbon properties, and presence of by-products throughout the regeneration process were scarcely considered. Furthermore, the regeneration of GAC saturated in organochlorine compounds has been barely analysed in the literature.

Among these organochlorine compounds, 124-TCB is used in many industrial processes, including the production of various pesticides (Blus, 2003; Jayaraj et al., 2016), POPs commonly found in the environment. The reduction of this compound has been studied using different oxidants. Barbash et al. (2006) indicated that persulfate could be an effective oxidiser of 1-24-TCB. In a previous work, thermally activated persulfate (TAP) was successfully applied to regenerate a spent GAC saturated in 124-TCB (Sanchez-Yepes et al., 2022). Also, the Fenton reaction has been successfully applied to treat 124-TCB. In this sense, Lorenzo et al. (2019) studied the removal of chlorobenzenes using hydroxylamine, goethite, and hydrogen peroxide to remove 124-TBC from polluted groundwater. In the same way, the abatement of 124-TCB using hydrogen peroxide and monochromatic light to activate (Lorenzo et al., 2021) or an iron complex (Conte et al., 2022) was effectively applied.

In the present work, the regeneration of GAC saturated with 124-TCB was studied by using H_2O_2 as oxidant and immobilised iron as catalyst. The influence of iron adsorbed and temperature on the regeneration of spent GAC with 124-TCB using H_2O_2 as the oxidant will be studied. The stability of GAC in the different adsorption-regeneration cycles and the unproductive consumption of the oxidant will be analysed, and the effect of the treatment on the chemical and physical properties of GAC will be fully examined. To our knowledge, this is the first study of the regeneration of GAC saturated in chlorobenzenes with adsorbed iron and hydrogen peroxide. Moreover, the effect of temperature on GAC

regeneration and the unproductive oxidant with this treatment is analysed for the first time.

2. Material and methods

2.1. Materials

The COC selected as the model pollutant, 124-TCB, is a semivolatile compound with moderate water solubility (28 mg L^{-1}) at room temperature (Schroll et al., 2004; Lorenzo et al., 2019, 2021). Analytical grade 124-TCB was purchased from Sigma-Aldrich. The calibration curves were prepared by dissolving pure 124-TCB in *n*-hexane. Bicyclohexyl was used as an internal standard (ISTD). A 35% v/v hydrogen peroxide solution was used as the oxidizing agent, iron (II) sulphate, $FeSO_4{\cdot}7H_2O$, was used as catalyst and titanium (IV) oxysulphate was used to quantify H_2O_2 concentration. Sodium carbonate, sodium bicarbonate, sulfuric acid, and acetone were used to determine the concentrations of chloride and short-chain organic acids by ion chromatography. The above compounds were analytical reagent grade and supplied by Sigma-Aldrich. Commercial GAC before pre-treatment (GAC-O) presented a surface area of 905 $m^2\ g^{-1}$ and a total pore volume of 0.42 $cm^3\ g^{-1}$ (Sanchez-Yepes et al., 2022).

2.2. Experimental procedure

2.2.1. GAC pre-treatment: acidic washing and iron adsorption

10 g of GAC-O was washed in 1 L of an acid water solution (pH = 3, adjusted with H_2SO_4) for 2 h (GAC-W). Subsequently, GAC-W was filtered and rinsed with H_2O milliQ and dried in an oven at 50 °C for 24 h.

1 g of GAC-W was put in contact with 5 g of an aqueous solution of cation Fe (II) at different concentrations from 7.16 to 89.52 mM, adjusted at pH_0 = 2.5. The biphasic mixture was agitated for 72 h, and the GAC with iron (GAC-Fe) was recovered by filtration and dried at 50 °C for 24 h. The remaining Fe (II) in the aqueous solution was quantified, and the iron adsorbed on the GAC was determined by the mass iron balance.

2.2.2. 124-TCB adsorption

5 g of GAC-W or GAC-Fe was placed in a stainless-steel mesh and immersed in a 1 L closed flask with 800 mL H_2O Milli-Q. A mass of 3 g of 124-TCB was added as organic liquid phase and the flask was closed and shaken at 300 rpm for 72 h at room temperature (22 ± 2 °C). After that, the stainless steel was removed, rinsed with H_2O Milli-Q , and dried at 50 °C for 24 h. The remaining 124-TCB in the flask was extracted with 200 mL of *n*-hexane and quantified by GC-MS. The mass of 124-TCB adsorbed on GAC was calculated by mass balance. This procedure provided GAC saturated in 124-TCB without iron (GAC-S) and GAC saturated in 124-TCB with immobilised iron (GAC-Fe-S).

2.2.3. Oxidation experiments

GAC (GAC-W, GAC-Fe, GAC-S, and GAC-Fe-S) reacted with hydrogen peroxide in well-mixed batch reactors. A 50 mL Milli-Q water volume was put in contact with 250 mg of GAC confined in a stainless-steel mesh basket. The reaction temperature was controlled using an agitation and heating plate coupled with a temperature-PID controller (IKA *C*-MAG HS 7). Once the temperature was reached, the specific amount of H_2O_2 needed was added (zero reaction time).

Two sets of experiments were carried out. In the first set, the reaction between GAC-W and GAC-Fe with H_2O_2 was studied at H_2O_2 and GAC concentrations of 166 mM and 5 g L^{-1} respectively, at two different temperatures (20–60 °C), for 180 min. The experimental conditions are described in Table SM1. Experiments B1 and B2 were carried out using GAC-W, while runs B3–B4 were performed using GAC-Fe-12 (12 $mg_{Fe}{\cdot}g_{GAC}^{-1}$). To check the catalytic role of adsorbed iron, GAC-Fe was filtered after run B4 and the solid was put in contact with a new H_2O_2 aqueous solution. This procedure was repeated three times.

The second set of experiments used GAC-S and GAC-Fe-S. The operation conditions are summarised in Table SM2. This set of experiments was designed to modify only one variable in each run to determine the effect of the studied variable avoiding the coupling effect of the variables. Runs R1 and R2 were carried out in the absence of adsorbed Fe and runs R3 to R7 were carried out at different concentrations of iron adsorbed (2–12 $mg_{Fe}{\cdot}g_{GAC}^{-1}$) and 20 °C. Runs 7 to 10 were carried out at different temperatures (20–80 °C) but using the same adsorbed iron (12 $mg_{Fe}{\cdot}g_{GAC}^{-1}$). The initial pH was 7. All runs were carried out at C_{GAC} = 5 g L^{-1} and $C_{H2O2,0}$ = 166 mM for 180 min (molar ratio H_2O_2:124-TCB of 20:1). The experiments were performed in triplicate. The data are expressed as the mean ± standard deviation.

The stoichiometry of the mineralization of 124-TCB with hydrogen peroxide is given by Eq. (1).

$$C_6H_3Cl_3 + 12{\cdot}H_2O_2 \rightarrow 6{\cdot}CO_2 + 12{\cdot}H_2O + 3{\cdot}HCl \quad (1)$$

60% excess with respect to the stoichiometric molar ratio H_2O_2:124-TCB required for complete 124-TCB mineralization (according to Eq (1)) was used in the experiments summarised in Table S2. The recovery of the adsorption capacity (RAC) was calculated according to Eq. (2).

$$RAC = \left(\frac{w_{124-TCB_{adsorbed}} / w_{GAC}}{q_{124-TCB_o}} \right) \cdot 100 \quad (2)$$

Being $w_{124\text{-}TCB,adsorbed}$ the mass of 124-TCB adsorbed after GAC regeneration, w_{GAC} the mass of GAC regenerated and $q_{124\text{-}TCBo}$ the adsorbed 124-TCB on GAC before the first GAC regeneration treatment. Furthermore, three consecutive cycles of adsorption-regeneration were carried out under the experimental conditions of R9. The experiments were performed in triplicate. The data are expressed as the mean ± standard deviation.

2.3. Analytical methods

124 − TBC in hexane was quantified by gas chromatography (Agilent 6890 N) with a Mass Spectrometry Detector (GC-MS). A HP-5MS chromatography column (30 m × 0.25 mm ID x 0.25 μm) was used as stationary phase and a constant flow rate of 1.7 $mL{\cdot}min^{-1}$ of helium as a mobile phase. 1 μL of the liquid sample was injected at a port temperature of 250 °C. The chromatographic oven worked under a programmed-temperature gradient, starting at 80 °C and increasing the temperature at a rate of 18 $°C{\cdot}min^{-1}$ up to 180 °C, then keeping it constant for 15 min. The H_2O_2 concentration was determined by colourimetry, reacting each sample with titanium (IV) oxysulphate and measuring the colour change by using a 410 nm spectrophotometer (BOECO S-20 VIS). Chloride and short-chain organic acids were determined by ion chromatography (Metrohm 761 Compact IC) with anionic chemical suppression and a conductivity detector. The pH was measured with a Basic 20-CRISON pH electrode. The iron content in the aqueous solutions was measured by spectroscopy of atomic emission (AES MP-4100 Agilent Technology) at a wavelength of 259.94 nm and a nebulizer pressure of 100 kPa. The total organic carbon (TOC) was measured using a Shimadzu TOC-V CSH analyser by oxidative combustion at 714 °C accomplished with a CO_2 infrared detector.

The toxicity of aqueous phase samples after regeneration/adsorption cycles was determined using the Microtox M500 analyser (Azur Environmental) using standard bioassays following the Microtox test protocol (ISO 11348–3, 2009). The test was conducted based on the bioluminescence inhibition of Vibrio Fischeri bacteria when exposed to toxic substances. The method was tested at 15 °C and 15 min exposure. The pH of the samples was fixed at 6–7, and the oxidant was neutralised with sodium thiosulfate to conduct the measures. The toxicity was expressed as toxicity units of the aqueous phase (TUs) calculated with Eq. (3) (Santos et al., 2004) where IC_{50} was the sample dilution ratio that

yields a 50% reduction of bacteria light emission calculated by Eq. (4).

$$TUs = \frac{100}{IC_{50}(\%)} \quad (3)$$

$$IC_{50}(\%) = \frac{V_{sample}}{V_{total}} 100 \quad (4)$$

Where V_{sample} is the volume of the polluted sample and V_{total} the volume sum of the sample volume and the added volume of the diluent and the bacteria.

The porous texture of the GAC was characterised by N_2 adsorption-desorption at −196 °C. The samples were outgassed at 150 °C for at least 8 h. From the N_2 isotherm, the apparent surface area (A_{BET}) was determined by applying the BET equation. The t-method allows obtaining the values of the external surface area (A_t) and the micropore volume (V_t). The mesopore volume (V_{mes}) was determined as the difference between the adsorbed volume of N_2 at a relative pressure of 0.99 (V_{tot}) and the micropore volume V_t. The surface chemistry of the sample was analysed by X-ray photoelectron spectroscopy (5700C model Physical Electronics) with Mg kα radiation (1253.6 eV). The maximum of the C1s peak was set to 284.5 eV and was used as a reference to shift the whole spectrum. Temperature-programmed desorption (TPD) was used to characterize the oxygen functional groups on the GAC surface formed during the different treatments. TPD analyses were obtained in a customised quartz fixed-bed reactor placed inside an electrical furnace and coupled to both a mass spectrometer (Pfeiffer Omnistar GSD-301) and to a non-dispersive infrared (NDIR) gas analyser (Siemens ULTRAMAT 22), to quantify CO and CO_2 evolution (calibration error <1%). In these experiments, c. a. 50 mg of the GAC was heated from room temperature to 930 °C at a heating rate of 10 °C·min^{-1}, in nitrogen (purity 99.999%, Air Liquide) flow (200 cm^3·STP·min^{-1}).

3. Results and discussions

3.1. Iron adsorption

The adsorption of Fe (II) on the GAC-W surface was studied using different iron cation concentrations in the aqueous phase ($C_{Fe\ (II)}$ = 7.16 to 89.52 mM) at a controlled temperature (22 ± 2 °C) for 72 h to ensure the equilibrium was reached, according to the procedure explained in the experimental section. The Fe (II) adsorbed on GAC was calculated from the iron mass balance of Fe (II) in the aqueous phase before and after Fe (II) adsorption. The obtained adsorption isotherm of Fe (II) on the GAC-W surface is shown in Figure SM1, which exhibits a typical Langmuir isotherm. The corresponding Langmuir parameters are summarised in Eq. (5), and the statistical parameters are inserted in Figure SM1. From the asymptotic value of the Langmuir isotherm, the saturation amount of Fe (II) adsorbed on the GAC surface was 12.56 $mg_{Fe}·g^{-1}_{GAC}$. The GAC samples with iron adsorbed have been named GAC-xFe (x the iron content in $mg_{Fe}·g^{-1}_{GAC}$).

$$q_{Fe} = \frac{12.56 \cdot 0.0053 \cdot C_{Fe}}{1 + 0.0053 \cdot C_{Fe}} \quad (5)$$

3.2. Effect of adsorbed Fe on 124-TCB adsorption

Incorporation of iron onto the GAC surface can affect the adsorption of pollutant (Huling and Hwang, 2010). The amount of 124-TCB adsorbed on GAC-W was 350 $mg_{124\text{-}TCB}·g^{-1}_{GAC}$ when the aqueous concentration of 124-TCB was 28 mg L^{-1} (solubility of 124-TCB in the aqueous phase at 28 °C) (Sánchez-Yepes et al., 2022). The effect of adsorbed Fe on 124-TCB adsorption has been investigated, and the results are presented in Figure SM2. As shown, the highest the amount of Fe adsorbed, the lower the 124-TCB adsorption. The adsorption of 124-TCB was reduced by 14% (300 $mg_{124\text{-}TCB}·g^{-1}_{GAC}$) when the GAC surface was saturated with 12 $mg_{Fe}·g^{-1}_{GAC}$. This fact agreed to reported by Huling and Hwang (2010). They observed that iron adsorbed on the GAC surface reduced the adsorption of methyl *tert*-butyl ether (MTBE), due to steric impediments.

3.3. Reactivity of GAC with H_2O_2

The reactivity of GAC-W with H_2O_2 with and without iron adsorbed was studied in runs B1–B4 (20 and 60 °C) (experimental conditions summarised in Table SM1). The conversion of H_2O_2 was calculated using equation (6).

$$X_{H_2O_2} = 1 - \frac{C_{H_2O_2}}{C_{H_2O_2,0}} \quad (6)$$

being $C_{H2O2,0}$ and C_{H2O2} the concentration of H_2O_2 at zero time and the corresponding reaction time, respectively. Oxidant conversion values are shown in Fig. 1.

As can be seen, H_2O_2 reacted with the GAC promoting the consumption of the oxidant (H_2O_2 conversion in the absence of GAC was less than 10% in the time interval studied, 3 h, at temperatures of 20 and 6 °C, data not shown). Furthermore, both the temperature and the surface of the presence of iron on the GAC increased the conversion of H_2O_2. A H_2O_2 conversion of 0.27 and 0.38 was obtained at 180 min and 20 °C, in the absence and presence of adsorbed iron, respectively. The corresponding oxidant conversion values at 60 °C were 0.6 and 0.8. As can be seen, the reaction rate of the hydrogen peroxide consumption decreased after 150 min. For this reason, 180 min was selected as the reaction time.

These results suggested that the presence of adsorbed iron on the surface of the GAC increased the reactivity of H_2O_2, as previously reported in literature (Moreno et al., 2007; Cabrera-Codony et al., 2015).

The GAC-12Fe after 180 min of reaction under the experimental conditions of run B4 (Table SM1), named GAC-12Fe–C1, was filtered and put in contact with an H_2O_2 aqueous solution (166 mM) at 60 °C for 180 min. This procedure was repeated two times, GAC-12Fe–C2 and GAC-12Fe–C3. The consumption of the H_2O_2 at each cycle is shown in SM4.

The results in Figure SM3 showed similar H_2O_2 conversions in the three cycles carried out under the conditions of run B4 (Table SM1), suggesting a catalytic behaviour of GAC-12Fe, which allows its use in successive runs. Furthermore, iron leaching in the aqueous phase was studied during the cycles shown in Figure SM3. The iron leached at each cycle was less than 0.5% of the initial iron adsorbed on GAC-12Fe. This result indicates that the prepared material is stable during successive cycles, and a homogeneous Fenton reaction does not occur.

3.4. Regeneration of GAC saturated in 124-TCB

The oxidation of adsorbed 124-TCB and the recovery of GAC adsorption capacity (RAC) has been studied at different temperatures (20–60 °C) and iron contents adsorbed on GAC. (0–12 $mg_{Fe}·g^{-1}_{GAC}$). The oxidant yield (Y_{Ox}) is defined as the mol of 124-TCB removed from the GAC surface per mol of H_2O_2 consumed. The removed 124-TCB is calculated as the readsorbed amount of 124-TCB after the spent GAC regeneration, using Eq. (7).

$$Y_{Ox} = \frac{mol_{124-TCB\ readsorbed}}{mol_{H_2O_2\ consumed}} \quad (7)$$

The $mol_{H2O2\ consumed}$ corresponds to the moles of H_2O_2 consumed in the GAC regeneration run and the $mol_{124\text{-}TCB\ readsorbed}$ are the moles of 124-TCB adsorbed after the regeneration with H_2O_2.

The recovery of adsorption capacity (RAC), oxidant conversion (X_{H2O2}) and oxidant yield (Y_{Ox}) after 180 min of reaction time have been calculated with Eqs. (2)–(4), respectively.

3.4.1. Effect of iron content adsorbed on the GAC

The effect of the adsorbed iron concentration on RAC, X_{H2O2} and Y_{Ox}

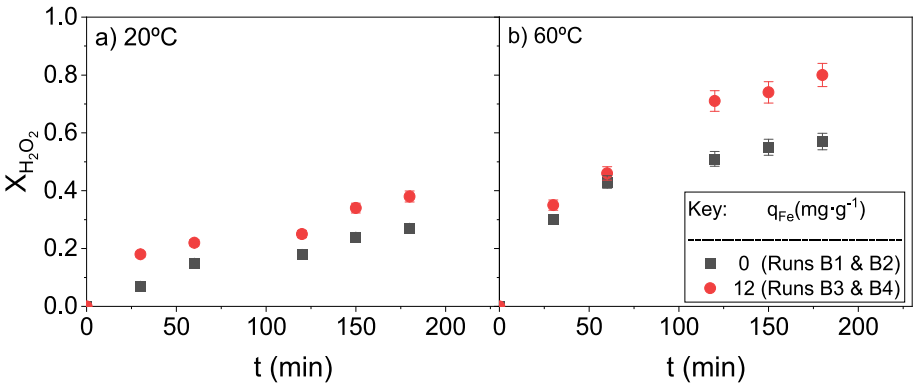

Fig. 1. H_2O_2 conversion by reaction with GAC-12Fe (runs B3 and B4) and GAC-W (runs B1 and B2) a) 20 °C and b) 60 °C, using $C_{H2O2,0}$ = 166 mM, C_{GAC} = 5 g L^{-1} and pH_0 = 7. Reaction conditions for runs B1 to B4 in Table SM1.

has been investigated at 20 °C in runs R1 and R3-R7 (Table SM2). RAC, YOx, and H_2O_2 conversion values are shown in Fig. 2. The effect of the adsorbed iron concentration on RAC, X_{H2O2} and Y_{Ox} has been investigated at 20 °C in runs R1 and R3-R7 (Table SM2). RAC, Y_{Ox} and H_2O_2 conversion values are shown in Fig. 2. The adsorbed iron concentrations (q_{Fe} values in Fig. 2) were obtained by placing contact solutions with different iron sulphate concentrations and GAC-W to reach equilibrium adsorption conditions. The amount of Fe adsorbed agreed with the Fe adsorption isotherm plotted in Figure SM1.

The higher the iron adsorbed, the higher the RAC value (Fig. 2a), which means that the oxidation of 124-TCB from GAC surface was improved. Oxidant consumption also increased with increased iron concentration adsorbed. On the other hand, the highest Y_{Ox} value (0.086 $mmol_{124\text{-TCB eliminated}}{\cdot}mmol^{-1}_{H2O2,\ reacted}$ is obtained at the highest amount of Fe adsorbed (12 $mg_{Fe}{\cdot}g^{-1}_{GAC}$). High Y_{Ox} values mean lower unproductive consumption of the oxidant and better efficiency of the oxidant in destroying the pollutant. Therefore, the best regeneration conditions correspond to12 $mg_{Fe}{\cdot}g^{-1}_{GAC}$. Moreover, the Y_{Ox} value of 0.083 $mmol_{124\text{-TCB eliminated}}{\cdot}mmol^{-1}_{H2O2,\ reacted}$ corresponds to the stoichiometric value for the total mineralization of 124-TCB (Eq. (1)).

Iron leaching was measured in the aqueous phases obtained in the regeneration runs shown in Fig. 2. In all cases, the iron leached was negligible (<1% of the initial amount of iron adsorbed), ensuring that the Fenton reaction took place heterogeneously on the GAC surface. The initial pH was 7, and the final pH of the reaction medium decreased and a value between 4 and 3.5. This pH reduction was in agreement with the formation of short acids in the reaction pathway. The lower iron concentration measured in solution (<0.2 $mg_{Fe}{\cdot}L^{-1}$) avoids the iron sludges produced in homogeneous Fenton Reagent, carried out at higher iron concentrations in the aqueous phase (usually much higher than the values allowed for Fe discharge). The initial pH of the oxidant aqueous solution does not need acidification when the iron is previously adsorbed on GAC, and the final pH is less acidic than that obtained after applying the Fenton Reagent with both iron and hydrogen peroxide in the solution.

The molar ratio of pollutant: oxidant: iron used in this work is 1:17:0.11. This ratio is similar to that employed by Huling and Hwang (2010) in the elimination of MTBE in GAC by iron amendment and Fenton oxidation (ratio 1:16.5:0.23) and Cabrera-Codony et al. (2015) studying the regeneration of AC saturated in octamethylcyclotetrasiloxane (1:20:0.023). On the contrary, Plakas and Karabelas (2016) applied a higher oxidant ratio to abate diclofenac adsorbed on Powered AC impregnated with iron oxide nanoparticles and H_2O_2. Regeneration of AC saturated in 2-chlorophenol by Huling et al. (2000) was also achieved using higher amounts (molar ratio pollutant:oxidant: iron 1: 63.7: 0.19).

3.4.2. *Effect of the reaction temperature*

The effect of reaction temperature on GAC regeneration was studied with GAC-12Fe–S in the range of 20–80 °C, using an oxidant concentration of 166 mM, neutral pH, and a GAC loading of 5 g·L^{-1}. The RAC, oxidant consumption and Y_{Ox} values obtained for each temperature (R7-R10 in Table S2) after 180 min of reaction are summarised in Fig. 3.

As shown in Fig. 3a and b, the higher the temperature, the higher the oxidant consumption, reaching values of 0.58 at 80 °C after 180 min of reaction time. The RAC values increased from 42% at 20 °C to 63% at 60 °C but did not increase further from 60 to 80 °C. The Y_{Ox} value shows a slight decrease from 20 to 60 °C (from 0.1 to 0.086 $mmol_{124\text{-TCB eliminated}}{\cdot}mmol^{-1}_{H2O2,\ reacted}$), but it presents a remarkable drop from 60 to 80 °C (from 0.086 to 0.064 $mmol_{124\text{-TCB eliminated}}{\cdot}mmol^{-1}_{H2O2,\ reacted}$). Therefore, increasing the temperature to 60 °C increases the pollutant oxidation on the GAC surface, but the highest temperatures produce remarkably unproductive oxidant consumption. Similar findings were also noticed in the literature on the Fenton reaction enhanced by temperature (Williams, 1928; McLane, 1949). Therefore, 60 °C is selected as the optimum temperature for the following experiments.

The H_2O_2 conversion found at 180 min and 60 °C in the absence of adsorbed 124-TCB (GAC-12FeC1, C2, C3 in Figure SM3) was approximately 0.80. The H_2O_2 conversion at the same operating conditions, but with 124-TCB adsorbed on GAC (GAC-12Fe–S in Fig. 3) was about 0.47. Therefore, it can be deduced that remarkably higher unproductive consumption of H_2O_2 takes also place in the absence of adsorbed pollutants adsorbed.

3.4.3. *Stability of the regenerated GAC*

Three cycles of spent GAC regeneration and 124-TCB adsorption was carried out with CAG-12Fe–S (q_{Fe} = 12 mg g^{-1}) at 60 °C with $C_{H2O2,0}$ = 166 mM, $C_{GAC\text{-}12Fe\text{–}S}$ = 5 g L^{-1} and pH = 7 (Run R9 in Table S2). After each regeneration cycle, the RAC, H_2O_2 consumption and Y_{Ox} were determined, and the results are summarised in Fig. 4. As shown, similar values of the RAC, oxidant consumption and Y_{Ox} are obtained in the three consecutive cycles (differences lower than 5% among them). These experimental results indicate that GAC with iron adsorbed can be used in stable cyclic operation with 124-TCB adsorption and adsorbent regeneration. In addition, the Y_{Ox} was kept in a value close to the stoichiometric value required for the 124-TCB mineralization, minimizing the unproductive consumption of the oxidant. The adsorption/regeneration mechanism of the GAC previously saturated with Fe can be summarised in Eqs. (8)–(11). In step 1, 124 TC B is adsorbed, after that in step 2, the H_2O_2 reacts with the adsorbed iron to produce the hydroxyl radicals, and this attacks to the 124-TCB which in several series reactions where oxidation produces are generated produces the regeneration of the GAC.

Step 1. 124-TCB adsorption

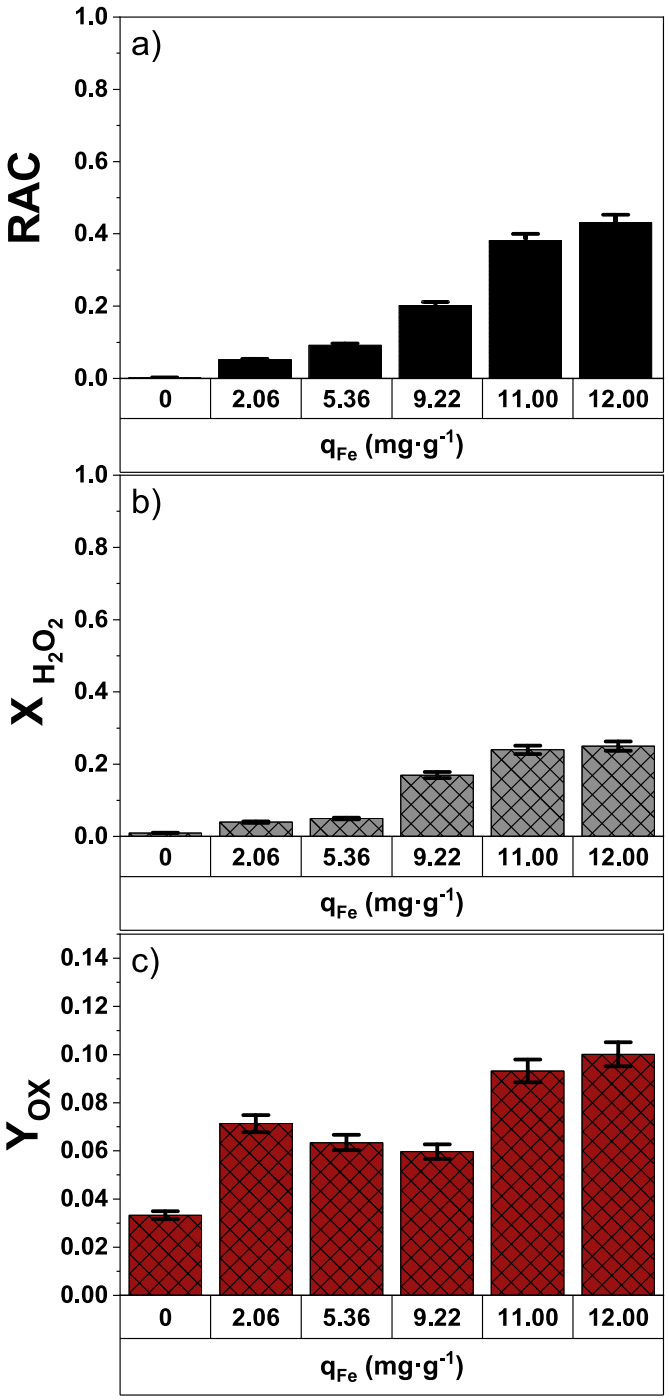

Fig. 2. Effect of adsorbed iron on a) recovered adsorption capacity (RAC), b) H_2O_2 conversion (X_{H2O2}) and c) oxidant yield (Y_{Ox}) in $mmol_{124\text{-}TCB\ eliminated} \cdot mmol^{-1}_{H2O2,\ reacted}$ at 180 min of reaction time, $C_{H2O2,0} = 166$ mM, $C_{GAC\text{-}xFe\text{-}S} = 5$ g L^{-1}, T = 20 °C, and neutral initial pH. The iron leached at each cycle was less than 0.5% of the initial iron adsorbed on GAC.

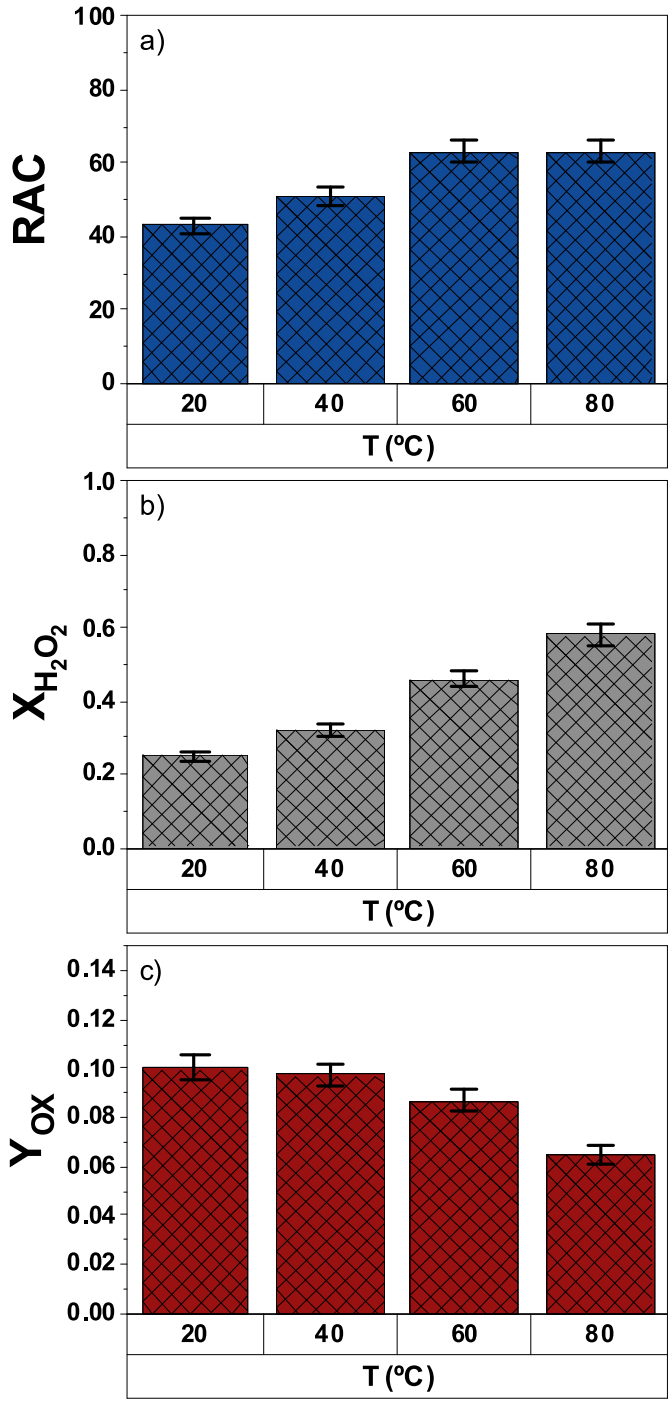

Fig. 3. Effect of temperature on a) recovery of Adsorption Capacity (RAC), b) H_2O_2 conversion (X_{H2O2}) and c) oxidant yield (Y_{Ox}) in $mmol_{124\text{-}TCB\ eliminated} \cdot mmol^{-1}_{H2O2,\ reacted}$ at 180 min of reaction time, $C_{H2O2,0} = 166$ mM, $C_{GAC\text{-}12Fe\text{-}S} = 5$ g L^{-1} and neutral initial pH. The iron leached at each cycle was less than 0.5% of the initial iron adsorbed on GAC.

$$TCB + GAC - Fe^{2+} \rightleftarrows GAC - Fe^{2+} - TCB \quad (8)$$

Step 2. Oxidation 124-TCB and GAC regeneration

$$GAC - Fe^{2+} - TCB + H_2O_2 \rightarrow GAC - Fe^{3+} - TCB + OH^{\bullet} + OH^{-} \quad (9)$$

$$GAC - Fe^{3+} - TCB + H_2O_2 \rightarrow GAC - Fe^{2+} - TCB + HO_2^{\bullet} \quad (10)$$

$$GAC - Fe^{2+} - TCB + OH^{\bullet} \rightarrow \rightarrow \rightarrow CO_2 + H_2O + HCl + GAC - Fe \quad (11)$$

The pH dropped from 7 to values between 4 and 3.5 at 180 min of regeneration time in the three cycles studied due to the presence of short-chain organic acids in the aqueous phase. At 180 min, only acetic acid was detected in the aqueous phase, with a concentration lower than 10 mg L^{-1}. Similar values of acetic acid concentration were found at the end of each regenerative cycle in the aqueous phase. The toxicity of the aqueous phase obtained after the regeneration cycle of the GAC was

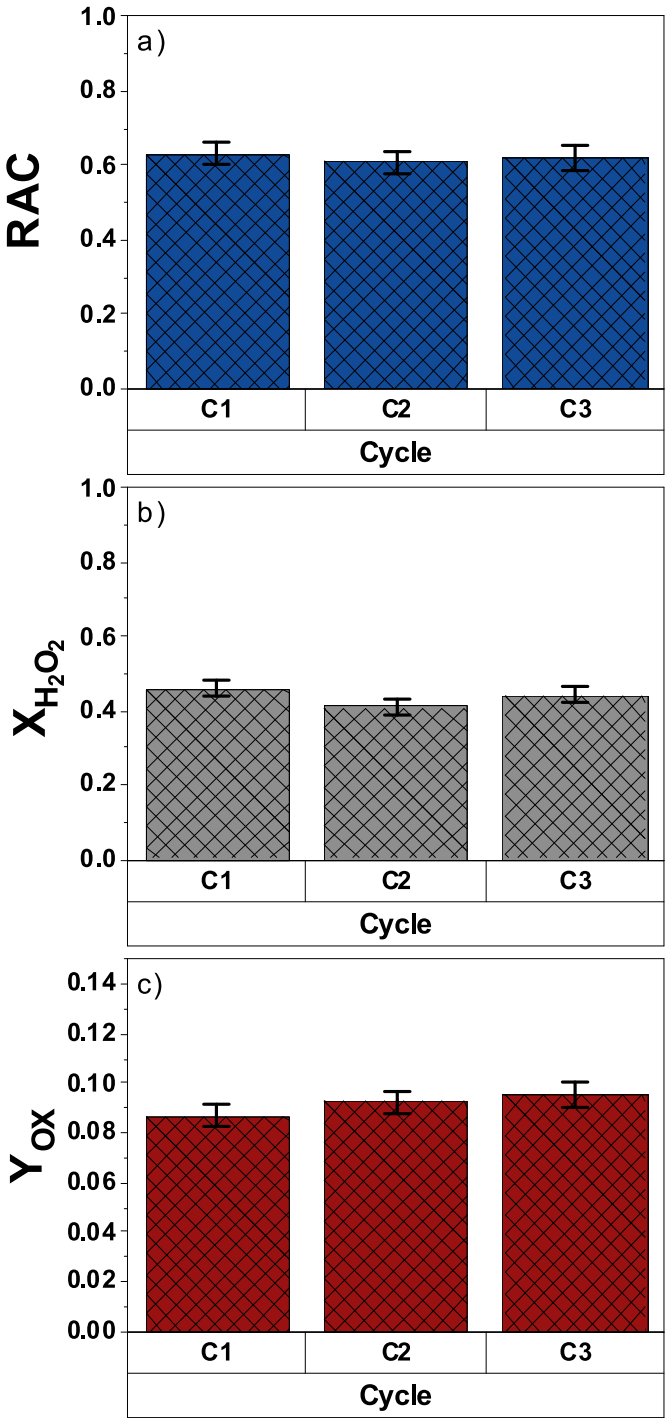

Fig. 4. Stability of GAC-12Fe in successive adsorption-regeneration cycles a) Recovery of Adsorption Capacity (RAC), b) H_2O_2 conversion (X_{H2O2}) and c) oxidant yield (Y_{Ox}) in $mmol_{124\text{-}TCB\ eliminated} \cdot mmol^{-1}_{H2O2,\ reacted}$ at 180 min, $C_{H2O2,0} = 166$ mM, $C_{GAC\text{-}12Fe\text{-}S} = 5$ g L^{-1}, T = 60 °C and neutral initial pH. The iron leached at each cycle was less than 1% of the initial iron adsorbed on GAC-12Fe.

measured. The initial TU of the water saturated with 124-TCB (28 mg L^{-1}) was 8.92, and negligible TU values were found in the aqueous phase obtained after the regeneration step, which meant the absence of the toxic by-products generated after regeneration treatment.

TOC was also measured at 180 min in the aqueous phase with values lower than 4 mg L^{-1}. Therefore, TOC in solution corresponds to 1% of the oxidised 124-TCB. Iron concentration was also measured in the aqueous phase at 180 min of each regeneration cycle with values lower than 0.1 mg L^{-1}. Iron leaching in the successive three regeneration cycles was less than 1% of iron adsorbed on the carbon.

3.5. Change in GAC physicochemical properties during adsorption-regeneration

The properties of the GAC surface can be modified after the adsorption-regeneration cycles. The characterisation of GAC after the different treatments is presented and discussed.

3.5.1. Effect of the acid pre-treatment, Fe and 124-TCB adsorption

The physicochemical properties of the original GAC (GAC-O) and GAC obtained after washing with acid water at pH = 3 (GAC-W) have been evaluated. The BET area, pore volume, atomic mass and acid group concentrations of GAC-O and GAC-W are summarised in Table 1. As shown, the surface area of GAC-O is 905 m^2 g^{-1}, being this value slightly reduced to 871 m^2 g^{-1} (6%) after the acidic pre-treatment (GAC-W). An equivalent reduction in the pore volume (7%) was observed in GAC-W. Kan et al. (Kan and Huling, 2009) after pre-treatment with acid water. Still, these authors also reported that acidic pre-treatment of GAC enhanced Fe sorption, avoiding the presence of amorphous and Fe precipitates that would be obtained with untreated GAC. The N_2 adsorption isotherms obtained for GAC-O and GAC-W are summarised in Figure SM4a, showing a type I isotherm (Thommes et al., 2015) attributed to a microporous material.

The effect of Fe adsorbed on the GAC surface has been studied with samples GAC-5Fe and GAC-12Fe. The results are also shown in Table 1 and Figure SM4a. As can be seen, GAC-5Fe and GAC-W have similar surface areas. The surface area of GAC-12Fe was about 7% lower than that of GAC-W. The N_2 adsorption isotherms of GAC-xFe show the same type I isotherm found for GAC-W, as shown in Figure SM4a. (Thommes et al., 2015), keeping the microporous structure.

Regarding the surface chemistry of GAC (Table 1), it was found that the atomic mass concentration of the GAC-O was mainly composed of oxygen (around 10%) and traces of N and S. In addition, TPD profiles were represented in Fig. 5 and the amount of CO and CO_2 obtained by TPD are given in Table 1. The CO and CO_2 amounts evidenced the low presence of surface carbon-oxygen groups. As can be seen in Fig. 5, CO_2 evolution is quite lower than that of CO for all the samples, evidencing the low presence of lactone, carboxyl and anhydride groups. As shown in Table 1 and Fig. 5, the amounts of CO and CO_2 slightly increased after washing (GAC-W), as evidenced by the significant decomposition of carbonyl and quinone groups as CO at high temperatures.

However, the adsorption of Fe promoted an increase of CO and CO_2 evolution (higher formation of oxygen surface groups). The comparison between CO profile for the GAC-W and GAC-12Fe samples (Fig. 5a) showed an increase in the CO desorption rate at high temperatures (around 870 °C). This increase was associated to the oxidation of the carbon surface by the sulphur species, which were incorporated into the carbon as part of the iron salts used in the pre-treatment. As reported in the literature, an AC containing sulphur species produces a higher C consumption than other functional groups present in the AC (Lin et al., 2021), however the extent of the carbon oxidation is not very significant, as can be seen in Table 1.

The C1s, O1s and Fe2p XPS spectra were represented in Figure SM5, and the atomic mass concentration is given in Table 1. The results of XPS analysis of GAC-5Fe and GAC-12Fe confirms the highest amount of adsorbed iron in GAC-12Fe. The results of XPS analysis of GAC-5Fe and GAC-12Fe confirms the highest amount of adsorbed iron in GAC-12Fe. With regard to Fe XPS spectra in Figure SM5c, amain peak in the Fe2p3/2 band was observed at 711.5 eV, which was associated to Fe (III) oxides such as FeOOH or Fe_2O_3. The S and O atomic content in the GAC surface increased after Fe adsorption because sulphate iron (II) salt was used to immobilise Fe on GAC.

The effect of 124-TCB adsorption on the physicochemical properties

Table 1
Physicochemical properties in the GAC samples tested.

Analytical technique	Adsorption		N_2 adsorption		XPS: mass surface concentration						TPD	
	q_{Fe} ($mg \cdot g^{-1}$)	Saturation in 124-TCB ($mg \cdot g^{-1}$)	A_{BET} ($m^2 \cdot g^{-1}$)	V_P ($m^3 \cdot g^{-1}$)	C (%)	N (%)	O (%)	S (%)	Fe (%)	Cl (%)	CO ($\mu mol \cdot g^{-1}$)	CO_2 ($\mu mol \cdot g^{-1}$)
GAC-O	0.00	0.00	908	0.420	88.82	0.25	10.60	0.33	0	0	290	18
GAC-W	0.00	0.00	851	0.380	90.59	0.51	8.75	0.15	0	0	349	41
GAC-5Fe	5.36	0.00	861	0.429	86.07	0.46	8.86	1.01	2.69	0	831	111
GAC-12Fe	12.00	0.00	806	0.408	58.59	0.65	28.05	4.32	8.40	0	1239	302
GAC-S	0.00	350	556	0.305	86.22	0.34	9.28	–	0	4.16	474	69
GAC-5Fe–S	5.36	330	662	0.338	77.67	0.31	14.85	–	4.88	2.29	564	108
GAC-12Fe–S	12.00	300	769	0.365	64.94	0.55	23.69	–	9.94	0.87	691	160
GAC-12Fe–C1	12.00	0.00	813	0.427	73.09	0.55	17.35	1.79	7.22	0	1050	263
GAC-12Fe–C3	12.00	0.00	761	0.411	66.86	0.62	20.66	1.93	9.93	0	1271	301
GAC-12Fe–*S*–C1-R	12.00	300	838	0.422	65.29	0.53	22.94	–	8.39	2.86	767	184
GAC-12Fe–*S*–C1–S	12.00	300	583	0.283	66.46	0.44	21.25	–	8.48	3.36	760	139
GAC-12Fe–*S*–C3-R	12.00	300	629	0.319	46.42	0.70	34.95	–	15.19	2.44	850	240
GAC-12Fe–*S*–C3–S	12.00	300	584	0.291	64.78	0.38	21.78	–	9.32	3.75	850	180

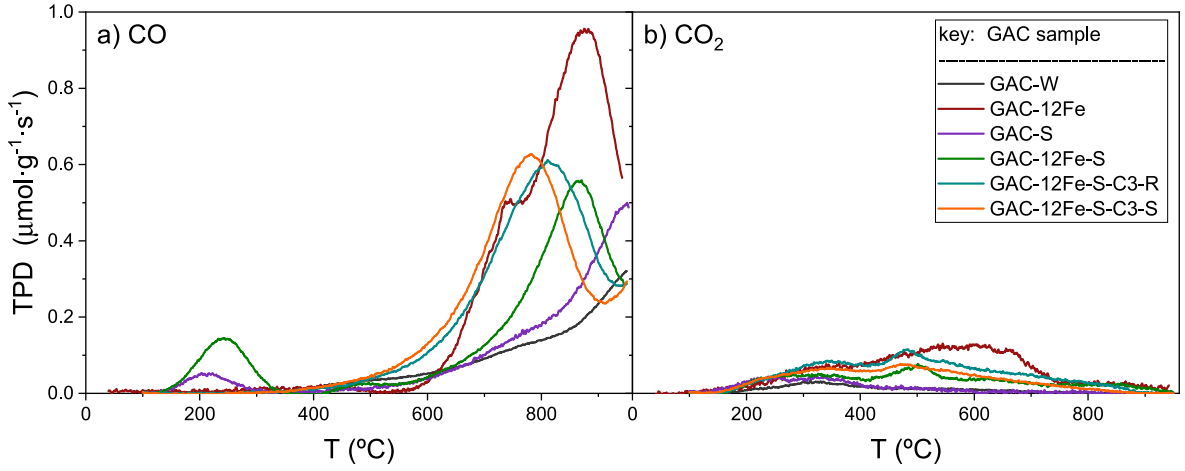

Fig. 5. TPD profile of GAC samples. a) CO desorption profile and b) CO2 desorption profile.

has been studied in the absence and presence of adsorbed iron. As shown in Table 1, the surface area of GAC-S was 35% lower than GAC-W. On the other hand, the reduction in surface area with GAC-5Fe–S and GAC-12Fe–S was 22% and 11%, respectively (related to the area of GAC-W). Therefore, the highest the amount of Fe adsorbed, the lower the reduction of the surface area after 124-TCB adsorption. This finding can be explained by considering that the amount of 124-TCB adsorbed on GAC increases as iron adsorbed decreases. As shown in Figure SM4b, the N_2 adsorption isotherms obtained after 124-TCB adsorption show a type I isotherm [46] again, keeping the microporous structure. As shown in Table 1, the evolution of CO and CO_2 during TPD decreases after 124-TCB. As shown in Fig. 5a, the amount of CO desorbed for GAC-12Fe–S is much lower than that obtained for GAC-12Fe. These results suggest that the adsorption of 124-TCB can reduce the sulphur species present on the carbon, decreasing the formation of carbon-oxygen complexes, which decompose at high temperatures (i.e. carbonyl, quinone groups …). On the other hand, a CO evolution was also observed at low temperature (around 200 °C), for saturated samples (GAC-S and GAC-12Fe–S), which corresponds to the desorption of the adsorbed pollutant (Berenguer et al., 2010).

As can be seen in Figure SM5a, C1s XPS spectra of the different samples were quite similar, only showing an increase of the intensity around 288.5 eV in the saturated samples, GAC-12Fe–S and GAC-12Fe–*S*–C3–S, which can be associated to the formation of carbonate groups or even to the interaction of *C*–Cl (https://xpsdatabase.com/). The O1s XPS spectra (in Figure SM5b) of both GAC-12Fe and GAC-12Fe–S showed a reduction of the oxygen surface concentration, probably due to the competitive adsorption of the contaminant and the sulphate species, due to relative Fe concentrations were quite similar.

3.5.2. *Effect of H_2O_2*

The physicochemical properties were characterised after the reaction of GAC with H_2O_2 at 60 °C. First, these changes are studied without adsorbed 124-TCB (samples GAC-12Fe–C1 and GAC-12Fe–C3 in Figure SM3). The apparent surface area, pore volume, atomic concentration on the GAC surface, and the evolved amounts of CO and CO_2 (TPD analysis) of the GAC-12Fe–C1 and GAC-12Fe–C3 samples are summarised in Table 1 and compared to the corresponding values obtained by GAC-12Fe. The N_2 adsorption-desorption isotherms are shown in Figure SM6. The surface area, pore volume and the surface chemistry of GAC after the reaction with the oxidant in the first (GAC-12Fe–C1) and third cycles (GAC-12Fe–C3) are very similar to the values determined for GAC-12Fe (before the reaction with the oxidant). These results confirm that the reaction between H_2O_2 and the GAC surface can be considered as a catalytic process with GAC surface not significantly oxidised or modified after the reaction with H_2O_2.

The GAC physicochemical properties have been studied during the adsorption-regeneration cycles of spent GAC-12Fe–S at 60 °C. The samples obtained after the first regeneration cycle, GAC12Fe–C1-R (regeneration of GAC-12Fe–S) and GAC-12-Fe-C1-S (resaturation of GAC-12Fe–C1-R with 124 TC B) and the samples obtained at the third regeneration cycle (GAC-12Fe–C3-R and GAC-12Fe–C3–S) have been analysed. The corresponding N_2 adsorption-desorption isotherms are depicted in Figure SM7, and the surface chemistry is summarised in Table 1. As shown in Figure SM7, the type of N_2 adsorption-desorption isotherms was unchanged with the adsorption-regeneration cycles, confirming that the microporous structure of the carbon was slightly affected by the adsorption-regeneration cycles. As summarised in Table 1, the surface GAC properties measured by GAC-12Fe–C1-R and GAC-12Fe–C3-R are similar to those obtained in GAC-12Fe, confirming the surface stability of the GAC during the regeneration process. Resaturation of the regenerated GAC with 124-TCB implies a reduction in the surface area (similar to the reduction observed between GAC-12Fe and GAC-12Fe–S). Still, the recovery of the surface area and surface chemistry after regeneration indicate that the oxidant reacted selectively with the 124-TCB, also confirmed by the reduction of chloride mass concentration on the GAC surface measured by the XPS technique. In addition, the regeneration treatment produced an increase of the relative oxygen surface concentration, which was reduced after the saturation cycle, remaining very stable during the successive cycles as can be seen in the XPS spectra in Figure SM5b. The type and quantity of oxygen groups on the surface were maintained. Furthermore, the TPD results revealed that the concentration of acidic groups on the GAC did not increase after the different regeneration/adsorption cycles, in agreement with a selective attack of H_2O_2 to the 124-TCB. As can be also seen in Fig. 5a, the profile for TPD-CO for GAC-12Fe–*S*–C3-R and GAC-12Fe–*S*–C3–S were quite similar to the one obtained for GAC-12Fe–S, indicating that the activated carbon remained stable during the consecutive oxidation and adsorption cycles.

The CO and CO_2 values measured by TPD for GAC-12Fe–C1R and GAC-12Fe–C2R were slightly lower than those obtained for GAC-12Fe–C1 and GAC-12Fe–C3, due to the presence of the remaining 124-TCB adsorbed on the GAC surface.

All these results evidence the high selectivity of this process to the pollutant, which maintains the physicochemical properties of the adsorbent (GAC) almost unchanging, facilitating its reuse in consecutive cycles of adsorption-regeneration.

4. Conclusions

In this work, the abatement of 124-TCB from polluted water has been successfully achieved using a two-step method. In the first step, the 124-TCB is adsorbed onto the GAC surface with Fe previously immobilised. The spent GAC is, then, regenerated by oxidising the adsorbed pollutant using hydrogen peroxide at a temperature of 60 °C. The adsorption/regeneration was carried out during three consecutive cycles, and the GAC remained stable during these successive cycles, maintaining 65% of the original adsorption capacity of the pollutant, without significant changes in the formation of oxygen surface groups, and amount of iron adsorbed. No aromatic or chlorinated by-products were detected in the aqueous phase obtained during the regeneration step, showing low TOC values. No toxic oxidation by-products were detected using the Microtox ® bioassay.

Although more research is required to implement this treatment on a full scale, this treatment is a promising technology to intensify the removal and destruction of organic pollutants. The tested method can be used to treat large volumes of polluted water, and the regeneration of GAC reduces the generation of highly contaminated solid waste. In addition, the use of immobilised iron did not require acidification of the final stream, avoiding the shortcomings of the Fenton reagent applied in a homogeneous process.

CRediT authorship contribution statement

Andrés Sánchez-Yepes: Methodology, Investigation, Writing – original draft. **Aurora Santos:** Funding acquisition, Resources, Conceptualization, Supervision. **Juana M:** Conceptualization, Investigation, Writing – original draft. **Rosas:** Conceptualization, Investigation, Writing – original draft. **José Rodríguez-Mirasol:** Funding acquisition. **Tomás Cordero:** Funding acquisition. **David Lorenzo:** Conceptualization, Methodology, Supervision, Writing – original draft.

Declaration of competing interest

The authors declare that they have no known competing financial interests or personal relationships that could have appeared to influence the work reported in this paper.

Data availability

No data was used for the research described in the article.

Acknowledgements

This work was supported by the EU LIFE Program (LIFE17 ENV/ ES /000260), the Regional Government of Madrid, through the CARESOIL project (S2018/EMT-4317), and the Spanish Ministry of Economy, Industry, and Competitiveness, through project PID 2019-105934RB-I00. A.S.-Y. would also like to thank Ministry of Science and Innovation for the support for predoctoral contracts under FPI grant PRE 2020-093195. This research was also supported by the Spanish Ministry of Science, Innovation and Universities and Junta de Andalucía through RTI 2018-097555-B-I00 and UMA18- FEDERJA-110 projects, respectively.

Appendix A. Supplementary data

Supplementary data to this article can be found online at https://doi.org/10.1016/j.chemosphere.2023.140047.

References

Alben, K., Belfort, G., Benedek, A., Frick, B.R., McGinnis, F.K., Pirbazari, M., Rosene, M. R., Shpirt, E., Tien, C., Weber, W.J., 1983. Treatment of water by granular activated carbon - discussion-ii - modeling and competitive adsorption aspects. Adv. Chem. 269–276.

Anfruns, A., Montes-Morán, M.A., Gonzalez-Olmos, R., Martin, M.J., 2013. H2O2-based oxidation processes for the regeneration of activated carbons saturated with volatile organic compounds of different polarity. Chemosphere 91, 48–54. https://doi.org/10.1016/j.chemosphere.2012.11.068.

Baghirzade, B.S., Zhang, Y., Reuther, J.F., Saleh, N.B., Venkatesan, A.K., Apul, O.G., 2021. Thermal regeneration of spent granular activated carbon presents an opportunity to break the forever PFAS cycle. Environ. Sci. Technol. 55, 5608–5619. https://doi.org/10.1021/acs.est.0c08224.

Barbash, A.M., Hoag, G.E., Nadim, F., 2006. Oxidation and removal of 1,2,4-trichlorobenzene using sodium persulfate in a sorption-desorption experiment. Water Air Soil Pollut. 172, 67–80. https://doi.org/10.1007/s11270-005-9052-3.

Bembnowska, A., Pełech, R., Milchert, E., 2003. Adsorption from aqueous solutions of chlorinated organic compounds onto activated carbons. J. Colloid Interface Sci. 265, 276–282. https://doi.org/10.1016/S0021-9797(03)00532-0.

Berenguer, R., Marco-Lozar, J.P., Quijada, C., Cazorla-Amorós, D., Morallón, E., 2010. Comparison among chemical, thermal, and electrochemical regeneration of phenol-saturated activated carbon. Energy Fuels 24, 3366–3372. https://doi.org/10.1021/ef901510c.

Blus, L.J., 2003. Organochlorine pesticides. Handbook of ecotoxicology 2, 313–340.

Cabrera-Codony, A., Gonzalez-Olmos, R., Martín, M.J., 2015. Regeneration of siloxane-exhausted activated carbon by advanced oxidation processes. J. Hazard Mater. 285, 501–508. https://doi.org/10.1016/j.jhazmat.2014.11.053.

Cai, Q.Q., Wu, M.Y., Hu, L.M., Lee, B.C.Y., Ong, S.L., Wang, P., Hu, J.Y., 2020. Organics removal and in-situ granule activated carbon regeneration in FBR-Fenton/GAC process for reverse osmosis concentrate treatment. Water Res. 183, 116119 https://doi.org/10.1016/j.watres.2020.116119.

Chen, Q., Liu, H., Yang, Z., Tan, D., 2017. Regeneration performance of spent granular activated carbon for tertiary treatment of dyeing wastewater by Fenton reagent and hydrogen peroxide. J. Mater. Cycles Waste Manag. 19, 256–264. https://doi.org/10.1007/s10163-015-0410-y.

Conte, L.O., Dominguez, C.M., Checa-Fernandez, A., Santos, A., 2022. Vis LED photo-fenton degradation of 124-trichlorobenzene at a neutral pH using ferrioxalate as catalyst. Int. J. Environ. Res. Publ. Health 19. https://doi.org/10.3390/ijerph19159733.

Crincoli, K.R., Jones, P.K., Huling, S.G., 2020. Fenton-driven oxidation of contaminant-spent granular activated carbon (GAC): GAC selection and implications. Sci. Total Environ. 734, 139435 https://doi.org/10.1016/j.scitotenv.2020.139435.

Gramatica, P., Papa, E., 2007. Screening and ranking of POPs for global half-l ife: QSAR approaches for prioritization based on molecular structure. Environ. Sci. Technol. 41, 2833–2839. https://doi.org/10.1021/es061773b.

Gramatica, P., Pozzi, S., Consonni, V., Di Guardo, A., 2002. Classification of environmental pollutants for global mobility potential. SAR QSAR Environ. Res. 13, 217. https://doi.org/10.1080/10629360290002695.

Horng, R.S., Tseng, I.-C., 2008. Regeneration of granular activated carbon saturated with acetone and isopropyl alcohol via a recirculation process under H2O2/UV oxidation. J. Hazard Mater. 154, 366–372. https://doi.org/10.1016/j.jhazmat.2007.10.033.

Huling, S.G., Arnold, R.G., Sierka, R.A., Jones, P.K., Fine, D.D., 2000. Contaminant adsorption and oxidation via Fenton reaction. Environ. Eng. 126, 595–600. https://doi.org/10.1061/(ASCE)0733-9372(2000)126:7(595).

Huling, S.G., Hwang, S., 2010. Iron amendment and Fenton oxidation of MTBE-spent granular activated carbon. Water Res. 44, 2663–2671. https://doi.org/10.1016/j.watres.2010.01.035.

Huling, S.G., Jones, P.K., Ela, W.P., Arnold, R.G., 2005. Fenton-driven chemical regeneration of MTBE-spent GAC. Water Res. 39, 2145–2153. https://doi.org/10.1016/j.watres.2005.03.027.

Huling, S.G., Ko, S., Park, S., Kan, E., 2011. Persulfate oxidation of MTBE- and chloroform-spent granular activated carbon. J. Hazard Mater. 192, 1484–1490. https://doi.org/10.1016/j.jhazmat.2011.06.070.

Jatta, S., Huang, S., Liang, C., 2019. A column study of persulfate chemical oxidative regeneration of toluene gas saturated activated carbon. Chem. Eng. J. 375, 122034 https://doi.org/10.1016/j.cej.2019.122034.

Jayaraj, R., Megha, P., Sreedev, P., 2016. Organochlorine pesticides, their toxic effects on living organisms and their fate in the environment. Interdiscipl. Toxicol. 9, 90–100. https://doi.org/10.1515/intox-2016-0012.

Kan, E., Huling, S.G., 2009. Effects of temperature and acidic pre-treatment on fenton-driven oxidation of MTBE-spent granular activated carbon. Environ. Sci. Technol. 43, 1493–1499. https://doi.org/10.1021/es802360f.

Klecka, G., Boethling, B., Franklin, J., Grady, L., Graham, D., Howard, P.H., Kannan, K., Larson, R.L., Mackay, D., Muir, D., van de Meent, D.M., 2000. Evaluation of Persistence and Long-Range Transport of Organic Chemicals in the Environment.

Li, X., Yang, C., Guo, J., Yang, J., Qiu, G., Yi, B., 2013. Regeneration of saturated activated carbon by Fenton reagent. Chin. J. Environ. 7, 3867–3873.

Lin, Y., Li, Y., Xu, Z., Guo, J., Zhu, T., 2021. Carbon consumption and adsorption-regeneration of H2S on activated carbon for coke oven flue gas purification. Environ. Sci. Pollut. Res. 28 https://doi.org/10.1007/s11356-021-14914-2.

Lorenzo, D., Dominguez, C.M., Romero, A., Santos, A., 2019. Wet peroxide oxidation of chlorobenzenes catalyzed by goethite and promoted by hydroxylamine. Catalysts 9. https://doi.org/10.3390/catal9060553.

Lorenzo, D., Santos, A., Sánchez-Yepes, A., Conte, L.Ó., Domínguez, C.M., 2021. Abatement of 1,2,4-trichlorobencene by wet peroxide oxidation catalysed by goethite and enhanced by visible LED light at neutral pH. Catalysts 11, 139. https://doi.org/10.3390/catal11010139.

Lougheed, T., 2007. Persistant organic pollutants - environmental stain fading fast. Environ. Health Perspect. 115, A20. https://doi.org/10.1289/ehp.115-a20. A20.

Ma, L., Wu, Z., He, M., Wang, L., Yang, X., Wang, J., 2020. Experimental study on Fenton oxidation regeneration of adsorbed toluene saturated activated carbon. Environ. Technol. 1–10 https://doi.org/10.1080/09593330.2020.1797891.

Marsh, H., Rodríguez-Reinoso, F., 2006a. Chapter 4 - characterization of activated carbon. In: Marsh, H., Rodríguez-Reinoso, F. (Eds.), Activated Carbon. Elsevier Science Ltd, Oxford, pp. 143–242. https://doi.org/10.1016/B978-008044463-5/50018-2.

Marsh, H., Rodríguez-Reinoso, F., 2006b. Chapter 8 - applicability of activated carbon. In: Marsh, H., Rodríguez-Reinoso, F. (Eds.), Activated Carbon. Elsevier Science Ltd, Oxford, pp. 383–453. https://doi.org/10.1016/B978-008044463-5/50022-4.

McLane, C., 1949. Hydrogen peroxide in the thermal hydrogen oxygen reaction I. Thermal decomposition of hydrogen peroxide. Chem. Phys. 17, 379–385. https://doi.org/10.1063/1.1747821.

Moreno, J.C., Sarria, V.M., Polo, Á.D., Giraldo, L., 2007. Evaluación del Peróxido de Hidrógeno en la Oxidación de Fenol con Hierro Soportado Sobre Tela de Carbón Activado. IT 18, 67–72. https://doi.org/10.4067/s0718-07642007000200010.

Peng, J., Wu, E., Wang, N., Quan, X., Sun, M., Hu, Q., 2019. Removal of sulfonamide antibiotics from water by adsorption and persulfate oxidation process. J. Mol. Liq. 274, 632–638. https://doi.org/10.1016/j.molliq.2018.11.034.

Plakas, K.V., Karabelas, A.J., 2016. A study on heterogeneous Fenton regeneration of powdered activated carbon impregnated with iron oxide nanoparticles. Glob. Nest. J. 18, 259–268. https://doi.org/10.30955/gnj.001894.

Rodan, B.D., Pennington, D.W., Eckley, N., Boethling, R.S., 1999. Screening of persistent organic pollutants: techniques to provide a scientific basis for POPs criteria in international negotiations. Environ. Sci. Technol. 33, 3488. https://doi.org/10.1021/es980060t.

Salvador, F., Martin-Sanchez, N., Sanchez-Hernandez, R., Sanchez-Montero, M.J., Izquierdo, C., 2015. Regeneration of carbonaceous adsorbents. Part I: thermal regeneration. Microporous Mesoporous Mater. 202, 259–276. https://doi.org/10.1016/j.micromeso.2014.02.045.

San Miguel, G., Lambert, S.D., Graham, N.J.D., 2002. Thermal regeneration of granular activated carbons using inert atmospheric conditions. Environ. Technol. 23, 1337–1346. https://doi.org/10.1080/09593332508618449.

Sanchez-Yepes, A., Santos, A., Rosas, J.M., Rodriguez-Mirasol, J., Cordero, T., Lorenzo, D., 2022. Regeneration of granulated spent activated carbon with 1,2,4-trichlorobenzene using thermally activated persulfate. Ind. Eng. Chem. Res. 61, 9611–9620. https://doi.org/10.1021/acs.iecr.2c00440.

Sánchez-Yepes, A., Santos, A., Rosas, J.M., Rodríguez-Mirasol, J., Cordero, T., Lorenzo, D., 2022. Regeneration of granulated spent activated carbon with 1,2,4-trichlorobenzene using thermally activated persulfate. Ind. Eng. Chem. Res. 61, 9611–9620. https://doi.org/10.1021/acs.iecr.2c00440.

Santos, A., Yustos, P., Quintanilla, A., García-Ochoa, F., Casas, J.A., Rodriguez, J.J., 2004. Evolution of toxicity upon wet catalytic oxidation of phenol. Environ. Sci. Technol. 38, 133–138. https://doi.org/10.1021/es030476t.

Santos, D.H.S., Duarte, J.L.S., Tonholo, J., Meili, L., Zanta, C.L.P.S., 2020. Saturated activated carbon regeneration by UV-light, H2O2 and Fenton reaction. Sep. Purif. Technol. 250, 117112 https://doi.org/10.1016/j.seppur.2020.117112.

Schroll, R., Brahushi, F., Dörfler, U., Kühn, S., Fekete, J., Munch, J.C., 2004. Biomineralisation of 1,2,4-trichlorobenzene in soils by an adapted microbial population. Environ. Pollut. 127, 395–401. https://doi.org/10.1016/j.envpol.2003.08.012.

Thommes, M., Kaneko, K., Neimark, A.V., Olivier, J.P., Rodriguez-Reinoso, F., Rouquerol, J., Sing, K.S.W., 2015. Physisorption of gases, with special reference to the evaluation of surface area and pore size distribution (IUPAC Technical Report). Pure Appl. Chem. 87, 1051–1069. https://doi.org/10.1515/pac-2014-1117.

Toledo, L.C., Silva, A.C.B., Augusti, R., Lago, R.M., 2003. Application of Fenton's reagent to regenerate activated carbon saturated with organochloro compounds. Chemosphere 50, 1049–1054. https://doi.org/10.1016/S0045-6535(02)00633-1.

Urano, K., Yamamoto, E., Tonegawa, M., Fujie, K., 1991. Adsorption of chlorinated organic compounds on activated carbon from water. Water Res. 25, 1459–1464. https://doi.org/10.1016/0043-1354(91)90175-.

Weber, W.J., Vanvliet, B.M., 1981. Synthetic adsorbents and activated carbons for water-treatment - overview and experimental comparisons. J. Am. Water Works Assoc. 73, 420–426.

Williams, B., 1928. The thermal decomposition of hydrogen peroxide in aqueous solutions. Trans. Faraday Soc. 24, 245–255.

Xiao, P.-f., An, L., Wu, D.-d., 2020. The use of carbon materials in persulfate-based advanced oxidation processes: a review. N. Carbon Mater. 35, 667–683. https://doi.org/10.1016/S1872-5805(20)60521-2.

Zhang, J., Zhang, N., Tack, F.M.G., Sato, S., Alessi, D.S., Oleszczuk, P., Wang, H., Wang, X., Wang, S., 2021. Modification of ordered mesoporous carbon for removal of environmental contaminants from aqueous phase: a review. J. Hazard Mater. 418, 126266 https://doi.org/10.1016/j.jhazmat.2021.126266.